Available online at **www.ijmrhs.com**

ISSN No: 2319-5886

International Journal of Medical Research & Health Sciences, 2017, 6(5): 38-48

150-Cavity Synchronization by Extended Loop in Neuraminidase of 2009 H1N1 Influenza Type A Virus: A Simulation Study

Sudha Singh, Anvita Gupta Malhotra, Mohit Jha, Khushhali M Pandey*

Department of Biological Science and Engineering, Maulana Azad National Institute of Technology, Bhopal, Madhya Pradesh, India

**Corresponding e-mail: kmpbiomanit@gmail.com; khushhalimenaria@manit.ac.in*

ABSTRACT

Neuraminidase (NA) is a novel drug target for antiviral inhibitors. In this druggable target, a cavity adjacent to the active site exists and is known as the 150-cavity. NA is divided into two groups: Group 1 and Group 2. The 150-cavity is present in Group 1 and absent in Group 2. Its behaviour is largely dependent on the nature of the 150-loop. H1N1 pandemic virus is believed to be an exception to this norm because it lies in Group 1 but doesn't contain the 150-cavity. Recent studies have shown that H1N1, also known as 2009N1, is capable of showing transition states that are characterized by different conformations of 150-loop. This 100-ns simulation study and subsequent analysis focused on identifying different conformations and develop an insight into the 150-loop which is directly responsible for transition states as well as 150-cavity formation. The study indicates direct regulating participation and involvement of a modified, extended 150-loop (144-156) in the formation of 150-cavity.

Keywords: Neuraminidase (NA), 2009 H1N1, 150-cavity, 150-loop, Influenza virus

INTRODUCTION

New antigenic subtypes arise from co-infection among different host species influenza viruses; the process being known as re-assortment. These new subtypes contribute to the emergence of human influenza pandemic flu and infect a significantly large population across the globe resulting in global outbreaks [1-7]. In 2009, the outbreak of H1N1 flu, also known as swine flu, resulted in a global crisis and public panic; thus, necessitating the need of medical attention for its effective treatment. The two major membrane glycoproteins associated with Influenza are Hemagglutinin (HA) and Neuraminidase (NA). Out of these two, HA is involved in disciplined fusion with sialic acid surface receptors which, in turn, facilitates the entry of the virus in the host cell; whereas NA cleaves the terminal sialic acid receptor linkage, thus facilitating the exit of virions [2].

The studies so far have indicated that NA is the most potential drug target for treatment of influenza infection. There are 9 subtypes (N1 to N9) of NA. Based on phylogenetic analysis, NA is divided into two groups, namely Group 1, having N1, N4, N5 and N8, and Group 2, having N2, N3, N6, N7 and N9, respectively. Previously, two FDA approved, rational structure based drugs Oseltamivir and Zanamivir were available as neuraminidase inhibitors (NAI) for Group 2 NA [8,9]. With building of resistance against these two drugs [10], their efficacy came down significantly and this was when a new drug called Laninamivir got developed. These drugs were not found to be efficient inhibitors for Group 1 NA. This lack of efficiency may owe its origin to the presence of 150-cavity adjacent to the active site [11]. This cavity, if taken into consideration, for developing a new promising molecule, is likely to provide higher specificity for Group 1 NA, as well as resistant strains. All known NAs contain a 150-loop with residues lying in the loop length range 147-152. The 150-loop has two conformations - an open conformation which leads to formation and consequent presence of 150-cavity, or a closed conformation which leads to an active site lacking 150-cavity [12].

The drug designing for H1N1 poses a tough challenge to the researchers, primarily becauseH1N1 shares the characteristics of group - 1 but does not have the 150-cavity. The 150-loop conformation plays an important role in substrate binding and high transmissibility of H1N1 in human beings. It also affects determination of specificity and

release of the product (sialic acid). It is speculated that 09N1 is akin to an intermediate state between typical Group 1 and Group 2 [13]. The 150-loop is discovered as the most dynamical motif which induces the inter-conversion of this loop among different conformations [14]. More insight into the 150-loop may confer some advantages to drug discovery process for H1N1.

In the present study, efforts have been made to understand the role played by 150-loop in the formation of 150-cavity of H1N1 through the 100-ns simulation. Taking a step size of 10 ns, simulated protein structures were used for the structural dynamics analysis of 150-loop and 150-cavity. The simulation shows that the well-known 150-loop (147-152) is not directly involved in the formation of 150-cavity due to its higher flexibility while the predicted extended 150-loop (144-156) is found to be directly involved in regulation of transition states (more open, open and closed) and controls the 150-cavity volumetric behaviour. The dynamics of extended 150-loop is important in the binding of ligands and is investigated to extract useful information for future potential drug design.

METHODOLOGY

Protein structure preparation

The crystal structure of neuraminidase with Oseltamivir (PDB ID: 3TI6) was retrieved from Protein Data Bank (PDB) [15]. The ligand from crystal structure was removed, protein was prepared and the resulting structure was used as the input for molecular dynamics (MD) simulations.

Molecular dynamics setup

MD simulations were achieved using GROMACS 5.0 [16,17]. The protein topology was generated by using pdb2gmx tool at standard pH 7 amino acid protonation state. G43a1 force field was used for the simulation. The input structure was solvated with the extended single-point charge (SPC) water model in a cubic box with 1.0 nm space around the solute. The net charge of the system was neutralized by replacing the water molecules with $3Na^+$ ions. The simulations involved 49,937 atoms, out of which 15,354 atoms belonged to water molecules. Energy minimization was done using steepest decent method. Following energy minimization, the system was equilibrated for 100 ps under NVT (constant number of particles, volume, and temperature), and NPT conditions (constant number of particles, pressure, and temperature) using leap-frog integrator. This was followed by an all - atom, molecular dynamics simulation for 100 ns.

The system was weakly coupled to an external bath using V-rescale thermostat. The reference temperature was set at 300 K and LINCS algorithm was used for bond constraints [18]. Long range electrostatic interactions were treated with Particle Mesh Ewald (PME) and the time step used was 2 fs [19].

GROMACS built-in tools were used for the determination of root mean square deviation (RMSD), root mean square fluctuation (RMSF), radius of gyration (Rg), to acquire more information about the stability of structure across the chosen time span of 100 ns.

Essential dynamics

Essential dynamics was performed using the entire trajectory to identify the global motions. Gromacs tools_g_covar and g_anaeig were used. Analysis was done using c-alpha atoms. The creation and subsequent diagonalization of the covariance matrix provided the Eigen vectors of interest. Porcupine plot was generated for the first eigenvector using PyMol [20]. Sausage plot was created using MD trajectory and the motion observed along eigenvector 1 was displayed using UCSF Chimera 1.10.2 software [21].

Prediction of cavity

Location of cavities and their volume was calculated using CASTp server [22].

Prediction of loop of NA

The 150-loop corresponding to different time scales was predicted by Teo-loop server (http://spin.ccic.ohio-state.edu/index.php/loop) [23].

RMSD based clustering analysis

This analysis was carried out by superimposition of different interval simulated structures through UCSF Chimera 1.10.2 software [21].

RESULTS AND DISCUSSION

Stability of the structure

Molecular dynamics simulation of neuraminidase was performed for a time period of 100 ns. Stability of the protein structure was analyzed using RMSD and Rg plots (Figure 1). The protein stabilized around 10 ns (10^4 ps) and remained stable till 100 ns (10^5 ps). The final RMSD value was found to be 0.329 nm. The average Rg value was determined as 1.95 nm [1.92 nm (min) – 1.98 nm (max)] and is an indication of the compactness of protein. Combining all this, the results point out that the simulated structures follow a stable trajectory. This is corroborated by the difference in RMSD and Rg values which is not of appreciable magnitude.

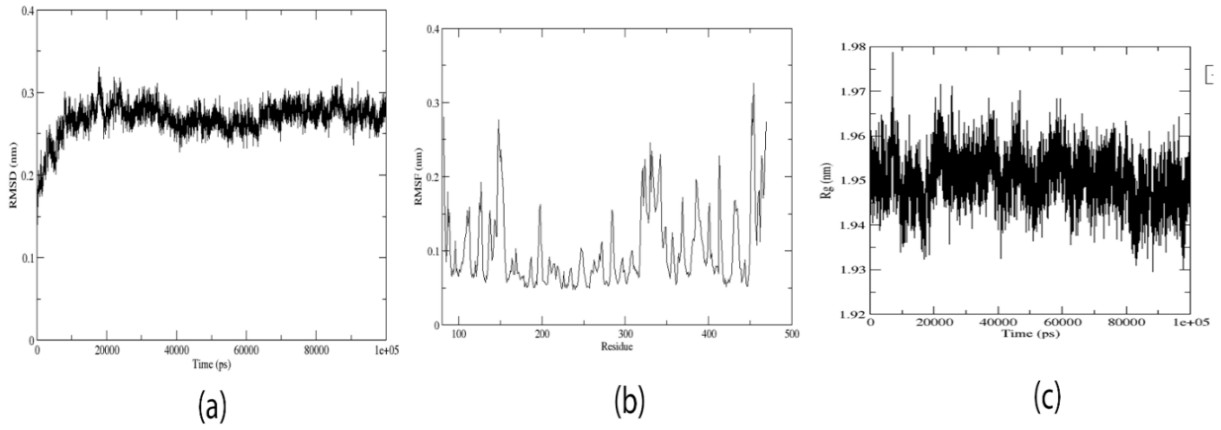

Figure 1 (a) RMSD (b) RMSF and (c) Rg plots for structural analysis of NA through Molecular Dynamics Simulations

Flexible and rigid regions of NA

The fluctuations of neuraminidase were analyzed using residue RMSF values. The RMSF profile identifies the flexible regions in the protein. Cα atoms were used for the calculation. The residues with RMSF of 0.15 nm and above were considered as mobile. Residues (Ser82, Val83, Gly87, Ser89, Ser110, Asp113, Ser125, Pro126, Leu127, Ala138, Gly147,Thr148, Ile149, Lys150, Asp151, Arg152, Ser153, Pro154, Pro197, Asp198,Ser 284, Ser319, Gly320, Ile321, Phe322, Gly323, Asp324, Asn325, Pro326, Asn329, Asp330, Lys331, Thr332, Gly333, Ser335, Cys336, Gly339, Pro340, Val341, Ser342, Ser343, Ser369, Gly385, Thr386, Asp387, Asn401, Gln412, Thr413, Gly414, Pro431, Lys432, Glu433, Asn435, Ser451, Asp452,Thr 453, Val454, Gly455, Pro459, Asp460, Gly461, Glu463, Leu464, Pro465, Phe466, Thr467, Ile468, Asp469) were found to be the mobile regions. A Sausage plot depicting the fluctuations during molecular dynamics simulations are shown in Figure 2. It also shows the correlation of sausage thickness with RMSF value.

The 150-loop flexibility

Group 1 NAs contain a 150-cavity (formed by amino acids 147-152 of the 150-loop) in their active site, whereas Group 2 NAs lack this cavity. In this analysis, the 150-loop residues (Gly147, Thr148, Ile149, Lys150, Asp151 and Arg152) RMSF values were found to be the higher than the chosen cut-off values. The 150-loop is thus found to exhibit a flexible nature.

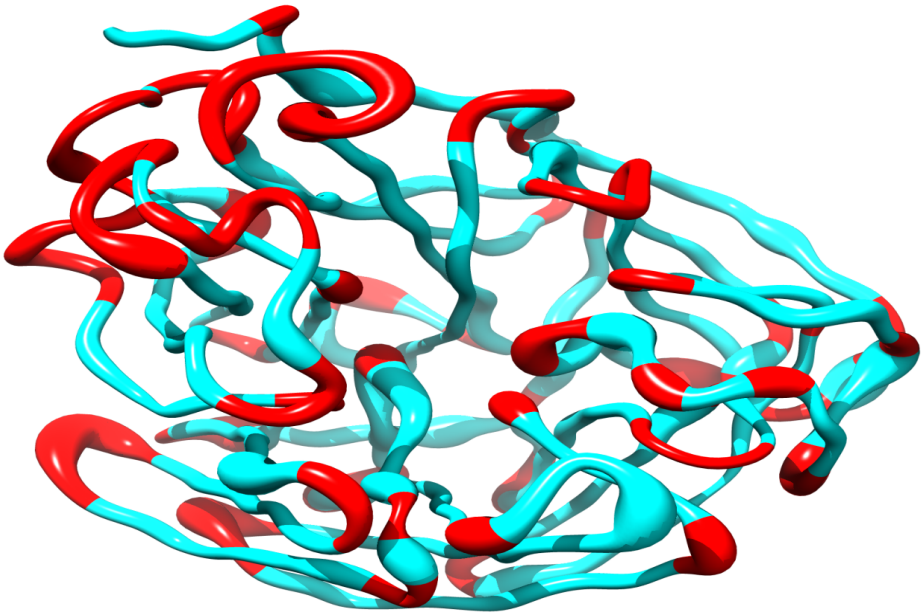

Figure 2 Sausage Plot showing the mobile regions computed from Eigen Vector 1. Coil in cyan and helix in red

Essential dynamics

Essential dynamics (ED) or principal component analysis (PCA) was done to identify the prominent characteristic motions in neuraminidase. Covariance matrix was constructed with a trace value of 16.22 nm^2. The top 20 eigenvectors contributed to 74% of the total mean square fluctuation. The porcupine plot highlighting the collective motions of the 150-loop and substrate binding pocket is shown (Figure 3).

It is observed that the shifts in the 150-loop are directed towards and away from the active site; the displacement of that loop shows high correlation with increasing and decreasing volume of active site.

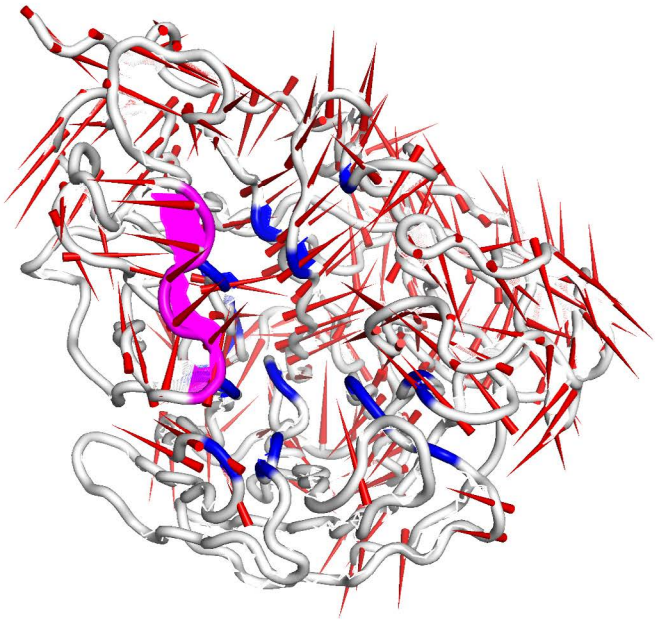

Figure 3 Porcupine plot shows collective motion of active site substrate binding pocket is coloured in blue and 150-loop in magenta

Prediction of loop of NA

The crystal structure of the 09N1 NA during MD simulations at different time scales revealed the different conformations of the 150-loop. The loop prediction at different time scales was carried out with the help of Teo-loop web server. This allowed the screening of average protein structures to develop better understanding of various roles played by loops in the context of protein-protein interactions and binding. All predicted loop categories were static with different loop lengths (Table 1). In this analysis, the loop length has been selected as 140-156, which was the range with the maximum frequency of occurrence during simulation. This selected loop (140-156) was used for further analysis.

Table 1 Decoding the mobility and time scales of protein loops description

Variables	00 ns	10 ns	20 ns	30 ns	40 ns	50 ns	60 ns	70 ns	80 ns	90 ns	100 ns
Start	140	140	141	147	147	136	147	147	140	140	140
End	156	156	156	155	156	155	156	156	155	156	156
Predicted loop category	static	static	static	static	static	static	static	static	static	static	static
Score1	-1.39	-1.41	-1.26	-0.59	-0.67	-1.11	-0.8	-0.99	-0.86	-1.43	-1.13
Score2	99.99	99.99	99.99	99.99	99.99	99.99	99.99	99.99	99.99	99.99	99.99
His frequency	0.06	0.06	0.06	0	0	0.05	0	0	0.06	0.06	0.06
Arg frequency	0.12	0.12	0.12	0.11	0.2	0.05	0.2	0.2	0.06	0.12	0.12
Lys frequency	0.12	0.12	0.12	0.11	0.1	0.1	0.1	0.1	0.12	0.12	0.12
Negative charged residue	0.12	0.12	0.12	0.11	0.1	0.1	0.1	0.1	0.12	0.12	0.12
Neutral residues	0.59	0.59	0.56	0.67	0.6	0.7	0.6	0.6	0.62	0.59	0.59
Secondary structure: bridge	0	0.06	0	0	0	0	0	0	0	0	0
3-10 helix	0.18	0	0	0	0	0	0	0	0	0	0
Hydrogen bond turn	0.47	0.29	0.12	0.22	0	0.15	0.2	0.2	0	0.35	0.18
Bend	0.06	0.29	0.25	0.33	0.4	0.65	0.4	0.4	0.62	0.29	0.47
Averaged solvent access	68.3	66.8	76.9	70.7	83.4	55.4	67.4	60.3	67.8	58.2	63.6
Averaged hydrophobicity	-1.8	-1.8	-2.2	-1.4	-1.7	-1.3	-1.7	-1.7	-1.7	-1.8	-1.8
Loop length	17	17	16	9	10	20	10	10	16	17	17
Loop contact sum	2214.6	2293.2	2184.4	1183.8	1355.7	2386.15	1373.03	1496.25	1971.76	2308.05	2144.7

Prediction of cavity

The active site prediction at different time intervals was done by CASTp server. The presence of 150-loop at adjacent active site is called 150-cavity. The maximum and minimum cavity volume values were found to be 797.1Å^3 and 203.2Å^3, respectively (Table 2).

Table 2 Predicted cavity volume and active site residues corresponding to different instants of time (150-loop residues are highlighted in bold)

Time	Voulme	Residues															
00ns	421.8	ARG118	GLU119	LEU134	**ASP151**	**ARG152**	**ARG156**	TRP178	SER179	ILE222	ARG224	THR225	GLN226	GLU227	VAL240	MET241	THR242
		GLY244	SER246	TYR275	GLU276	GLU277	CYS278	ARG292	ASN294	TYR406							
10ns	797.1	ARG118	GLU119	THR135	GLN136	**HIS144**	**ILE149**	**LYS140**	**ASP151**	**ARG152**	**SER153**	**TYR155**	**ARG156**	TRP178	ARG224	THR225	GLN226
		GLU227	SER246	GLU276	GLU277	ARG292	ASN294	LYS350	ARG371	TRP403	GLU405						
20ns	321.6	GLU119	PRO120	PHE121	LEU134	**ARG152**	**SER153**	**ARG156**	ALA177	TRP178	SER179	ALA180	GLU227	SER228	LYS350	TYR406	TRP423
30ns	487.2	ARG118	GLU119	GLN136	**ILE149**	**LYS150**	**ASP151**	**ARG152**	**SER153**	**TYR155**	**ARG156**	ALA177	TRP178	ILE222	ARG224	GLN226	GLU227
		VAL240	THR242	SER246	GLU276	GLU277	CYS278	SER179	ARG292	ASN294	THR225						
40ns	203.2	TRP178	SER179	ARG224	THR225	GLN226	VAL240	THR242	TYR275	GLU276	GLU277	CYS278	LYS350				
50ns	588.5	ARG118	GLU119	GLN136	**THR148**	**LYS150**	**ASP151**	**ARG152**	**SER153**	**TYR155**	**ARG156**	TRP178	SER179	ILE222	ARG224	THR225	GLN226
		GLU227	VAL240	MET241	THR242	SER246	GLU276	GLU277	CYS278	ARG292	ASN294						
60ns	491	ARG224	THR225	GLN226	GLU227	VAL240	THR242	TYR275	GLU276	GLU277	CYS278	LYS350					
70ns	319	GLU119	ARG152	TRP178	ILE222	ARG224	THR225	GLU226	GLU227	VAL240	THR242	SER246	TYR275	GLU276	GLU277	CYS278	ASN294

		LYS350	TYR406														
80ns	535.1	GLU119	PHE121	LEU134	**ILE149**	**LYS150**	**ASP151**	**ARG152**	**PRO152**	**TYR155**	**ARG156**	ALA177	TRP178	SER179	ILE222	ARG224	THR225
		GLN226	GLU227	SER228	VAL240	THR242	SER246	GLU276	GLU277	CYS278	VAL349						
90ns	616.4	ARG118	GLU119	PHE121	LEU134	**THR148**	**ASP151**	**ARG152**	**ARG156**	TRP178	SER179	ALA180	ILE222	ARG224	THR225	GLN226	GLU227
		VAL240	THR242	SER246	TYR275	GLU276	GLU277	CYS278	ARG292	ASN294	VAL349						
100ns	435.2	GLU119	**ASP151**	**ARG152**	**ARG156**	TRP178	SER179	ILE222	ARG224	THR225	GLN226	GLU227	VAL240	THR242	SER246	TYR275	GLU276
		GLU277	CYS278	ARG292	ASP294	LYS350	TYR406										

Analysis of regularity loop participation for formation of 150-cavity

Previous studies have established that the 150-loop is responsible for the open and close conformation of 150-cavity. However, loop regulation for the cavity formation is still unknown. This study has attempted to address this issue by correlating RMSD values of 150-loop (147-152) and modified loop (140-156) with cavity forming residues. The modifies loop was determined by leave one out method (described below).

Previously defined 150 – loop (147-152)

The role of 150-loop for predicting the regulation of 150-cavity formation on the active site of NA was investigated with the help of RMSD values. The cut-off was chosen as 1.0. The RMSD value less than 1.0 indicates the participation of 150-loop in the cavity at different time intervals. However, no definite relation is observed between the RMSD values, presence of loop and regulation of cavity formation. This indicates the flexible nature of the loop. The values obtained are shown in Table 3 and Figure 4. This indicates the need of a more thorough analysis into the role played by 150-loop in the regulation of 150-cavity formation.

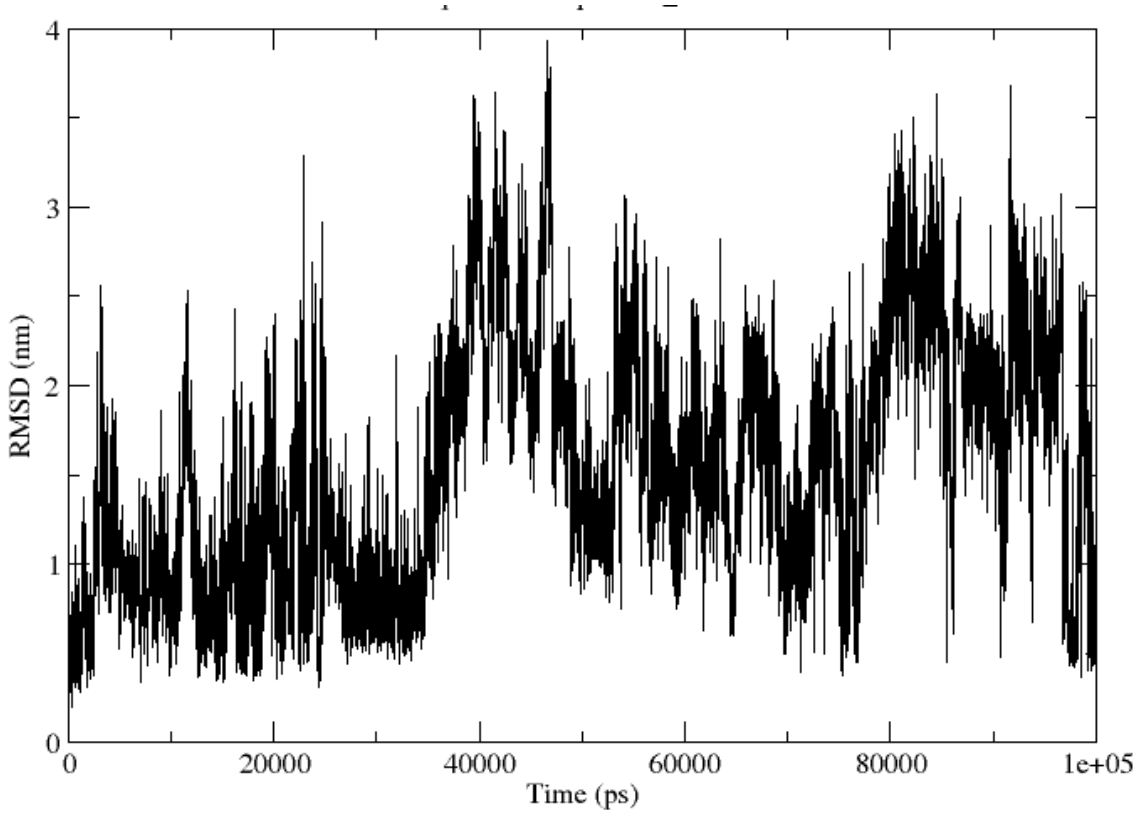

Figure 4 RMSD V/s Time Plots for representation of 150-loop (147-152) at different time intervals

Table 3 The relation between 150-loop (147-152) and 150-cavity through RMSD values and presence of loop residues

S.No	Different time frames	150-loop (147-152)		150-Cavity
		RMSD values	Presence of Loop residue in cavity	
1	00ns	0	151, 152	Present
2	10ns	0.43	149, 150, 151, 152	Present
3	20ns	1.21	152	Present
4	30ns	1.18	149, 150, 151, 152	Present
5	40ns	2.31	NA	NA
6	50ns	1.6	148, 150, 151,152	Present
7	60ns	1.85	NA	NA
8	70ns	1.14	152	Present
9	80ns	2.71	1,49,15,01,51,152	Present
10	90ns	1.91	148, 151, 152	Present
11	100ns	0.86	151, 152	Present

Predicted modified extended loop (140-156)

In the previously selected predicted loop (140-156), residues were replaced one by one with intact 150-loop (147-152) and the RMSD was calculated at each time interval to predict the relation between modified extended loop and existence of 150-cavity (Table 3). The relation showed by this extended loop (144-156) for 150-cavity prediction with 1.0 cut-off RMSD values is shown in Table 4 and Figure 5. When the RMSD of this extended 150-loop is higher than the cut – off, the loop does not participate in the formation of 150-cavity.

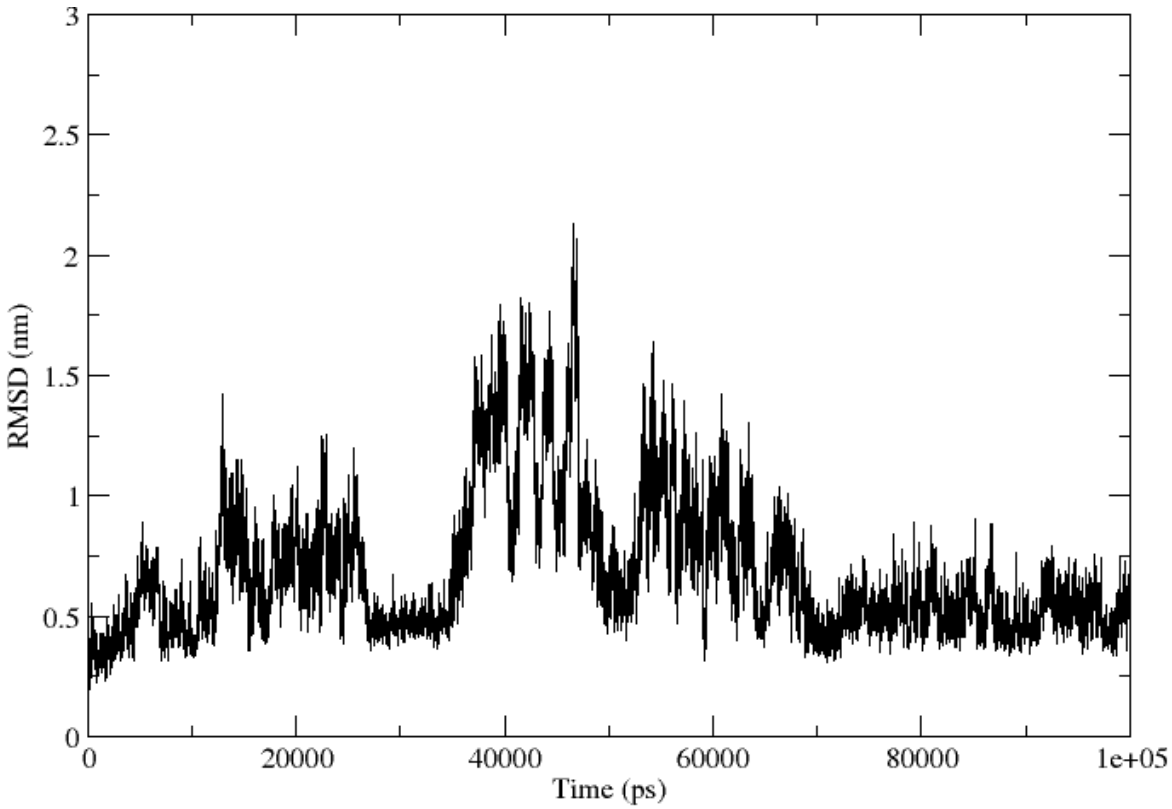

Figure 5 RMSD V/s Time Plots for representation of predicted extended loop (144-156) at different time intervals

Table 4 The relation of predicted modified extended loops RMSD with existence of 150-cavity

Time\loop length	150-cavity	(140-156)	(141-156)	(142-156)	(143-156)	(144-156)
00 ns	Present	0.0005129	0.0005198	0.000528	0.0005247	0.0005343
10 ns	Present	0.4	0.36	0.37	0.37	0.37
20 ns	Present	0.51	0.53	0.72	0.82	0.95
30 ns	Present	0.45	0.43	0.41	0.41	0.52
40 ns	NA	0.61	0.81	0.96	1.07	1.33
50 ns	Present	0.38	0.41	0.43	0.45	0.67
60 ns	NA	0.62	0.76	0.86	0.92	1.09
70 ns	Present	0.56	0.53	0.49	0.47	0.4
80 ns	Present	0.41	0.37	0.42	0.46	0.47
90 ns	Present	0.59	0.56	0.53	0.51	0.44
100 ns	Present	0.49	0.48	0.53	0.56	0.59

RMSD-based clustering analysis of extended loop (144-156)

To get more details of regulation of the 150-loop conformations enhanced by simulation, RMSD-based clustering analyses were carried out. Figure 6 depicts the initial structure and structures of cluster centres at different intervals. In the crystal structure, the presence of 150-loop usually forms the 150-cavity whereas absence of 150-loop turns away the 150-cavity from the binding pocket. This analysis provided us three distinct loop conformations. Whereas the first and second show the presence of 150-loop on the inner side in open and closed conformations respectively (Figure 6 a), the third one shows the absence of 150-loop on the outer side in a 'more open' conformation [14]. The first two types account for 80% of the total conformations while the remaining 20% falls under the third type.

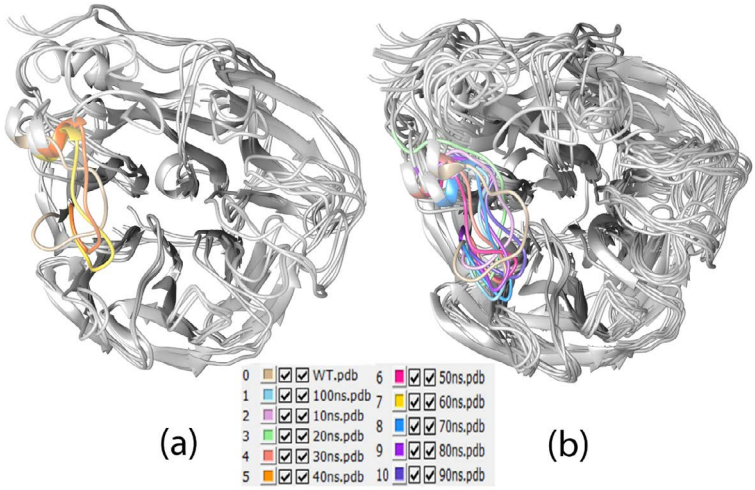

Figure 6 Superimposition of extended loop (144-156) structures obtained at different time intervals. (a) more open conformations (40 ns and 60 ns) (b)open and closed conformations (00 ns, 10 ns, 20 ns, 30 ns, 50 ns, 70 ns, 80 ns, 90 ns, 100 ns)

The starting structure (00 ns) of NA was closed and its volume was 421.8. Accordingly, a volume value higher than 421.8 corresponds to closed conformation whereas less than 421.8 corresponds to open conformation.

Out of the simulation results obtained, 80% support the role of extended loop (144-156) in the formation of 150-cavity. Out of this, 62.5% (10 ns, 30 ns, 50 ns, 80 ns, 90 ns) fall in open conformation whereas 37.5% (20 ns, 70 ns, 100 ns) fall under the closed conformation. In closed conformation, the extended loop length is: 151, 152/153,156. In open conformation, the extended loop length is: 144,149/148,150,151,152,153/154,155,156 in Table 5 and Figure 7. In open conformation, the presence of extended loop increases the volume of 150-cavity.

The remaining 20% are characterized by higher RMSD values and may correspond to a more open conformation. At 40 ns, the extended 150-loop is not present and there is an accompanying volume decrease. However, in case of 60

ns the extended 150-loop is not present but the volume increases. This could be attributed to contribution made by other residues.

Table 5 The relationship between the presence of extended loop residues and the volume of 150-cavity

S.No	Different time frames	Extended loop (144-156)		Cavity Volume	150-Cavity
		RMSD	Loop residue in cavity		
1	00 ns	0	15,11,52,156	421.8	Present
2	10 ns	0.37	144, 149,150,151,152,153,155,156	797.1	Present
3	20 ns	0.95	152, 153, 156	321.6	Present
4	30 ns	0.52	149, 150, 151, 152, 153, 155, 156	487.2	Present
5	40 ns	1.33	NA	203.2	NA
6	50 ns	0.67	148, 150, 151,152, 153, 155, 156	588.5	Present
7	60 ns	1.09	NA	491	NA
8	70 ns	0.4	152	319	Present
9	80 ns	0.47	14,91,50,15,11,52,15,40,00,000	535.1	Present
10	90 ns	0.44	148,151,152, 156	616.4	Present
11	100 ns	0.59	15,11,52,156	435.2	Present

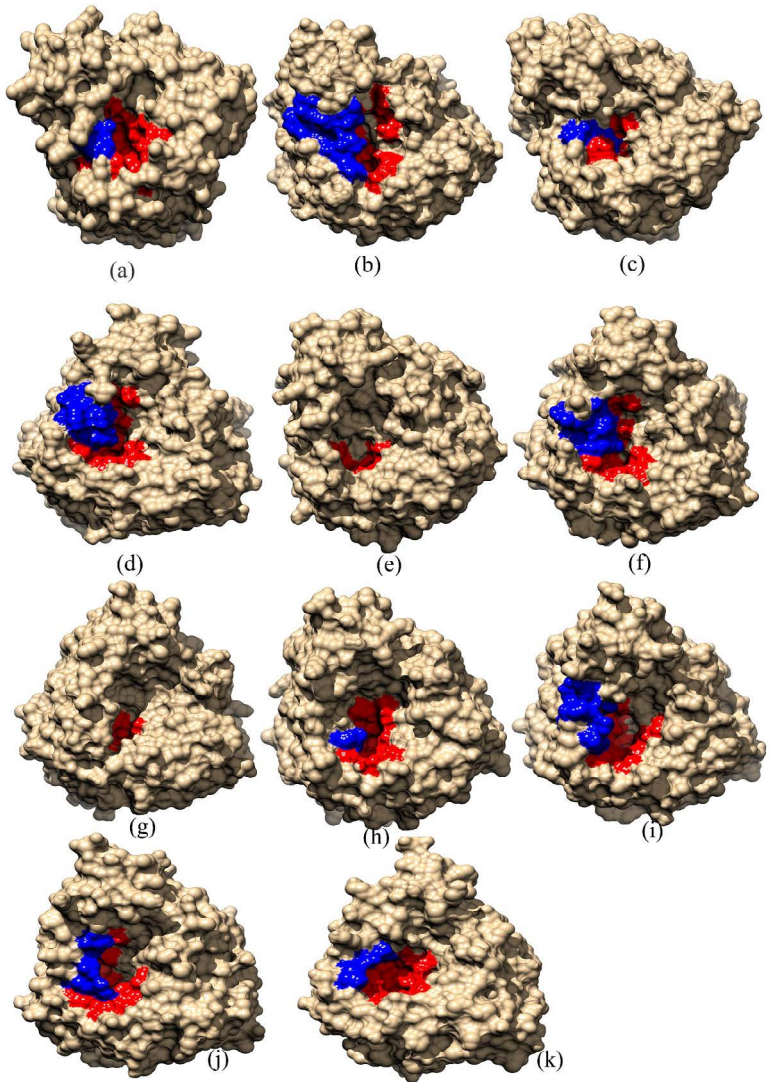

Figure 7 Comparisons of the molecular surfaces of presence of extended loop (blue) in the active-site(red) of NA (a) 00 ns (b) 10 ns (c) 20 ns (d) 30 ns (e) 40 ns (f) 50 ns (g) 60 ns (h) 70 ns (i) 80 ns (j) 90 ns (k) 100 ns

There are three types of conformations: closed, open, and more open conformation. The (144, 149/148, 150, 151, 152, 153/154, 155, 156) are combinations of both conformations used in structure-based drug design for targeting transition states.

CONCLUSION

In this study, the formation of 150-cavity was predicted using molecular dynamics method with the pre-set goal of exploring dynamic movement of the extended 150-loop (144-156). Despite the presence of 150-cavity in Group 1 NA, recent findings indicated that the structure of the 2009 pandemic H1N1 NA lacked 150-cavity. The simulation of H1N1 NA protein for 100 ns in this study indicated that in soluble environment the extended 150-loop regulates the appearance and disappearance of 150-cavity through volumetric variations.

The RMSD - based analysis of previously defined 150-loop (147-152) was found to be little inadequate as it did not directly regulate the formation of 150-cavity, thus necessitating the need of collecting more information about the involvement of loop in the regulation mechanism of the 150-cavity. The current study has focused on the extended loop that regulates the 150-cavity during conformational changes. Different conformations of protein were used for determination of the target loop with intact 150-loop during 100 ns simulation. The RMSD-based analysis was carried out by replacing loop residues one by one. The involvement of loop in the formation/regulation of 150-cavity was identified. This observed loop is found to have an extended 144-156 residue length, throughout the simulation.

It is found to be involved in direct regulation of the 150-cavity; though the nature of the regulation varies. The formation of 150-cavity depends on the conformation of the extended loop, 20% events resulted in more open conformations without the 150-cavity, 37.5% events resulted in closed loop conformation and the accompanying 150-cavity, whereas 62.5% events resulted in open loop conformation and accompanying 150-cavity. This suggests that residues from 149-156 of the extended loop play a significant role towards the appearance of the cavity and can, therefore, be used for novel drug molecule designing. This is likely to open new vistas of knowledge that can be effectively used to derive more potent ligand with novel scaffold in specific reference to the extended 150-cavity.

CONFLICT OF INTEREST

The authors declare that they have no conflict of interest.

ACKNOWLEDGEMENTS

The authors are thankful to Dr. Ajay Pandey, a faculty member at MANIT, Bhopal, for his help, support, and guidance.

REFERENCES

[1] Webster, Robert G., et al. "Evolution and ecology of influenza A viruses." *Microbiological reviews* 56.1 (1992): 152-179.
[2] Russell, Rupert J., et al. "The structure of H5N1 avian influenza neuraminidase suggests new opportunities for drug design." *Nature* 443.7107 (2006): 45-49.
[3] Cox, N. J., and K. Subbarao. "Global epidemiology of influenza: past and present." *Annual review of medicine* 51.1 (2000): 407-421.
[4] Guan, Yi, et al. "The emergence of pandemic influenza viruses." *Protein & cell* 1.1 (2010): 9-13.
[5] Sun, YePing, et al. "In silico characterization of the functional and structural modules of the hemagglutinin protein from the swine-origin influenza virus A (H1N1)-2009." *Science China Life Sciences* 53.6 (2010): 633-642.
[6] Liu, Di, et al. "Interspecies transmission and host restriction of avian H5N1 influenza virus." *Science in China Series C: Life Sciences* 52.5 (2009): 428-438.
[7] Gao, George F., and YePing Sun. "It is not just AIV: from avian to swine-origin influenza virus." *Science China Life Sciences* 53.1 (2010): 151-153.
[8] Von Itzstein, Mark. "The war against influenza: discovery and development of sialidase inhibitors." *Nature reviews Drug discovery* 6.12 (2007): 967-974.
[9] Colman, P. M. "Zanamivir: an influenza virus neuraminidase inhibitor." *Expert review of anti-infective therapy* 3.2 (2005): 191-199.
[10] Song, Min-Suk, et al. "Increased virulence of neuraminidase inhibitor-resistant pandemic H1N1 virus in mice: potential emergence of drug-resistant and virulent variants." *Virulence* 4.6 (2013): 489-493.
[11] Samson, Mélanie, et al. "Influenza virus resistance to neuraminidase inhibitors." *Antiviral research* 98.2 (2013): 174-185.

[12] Li, Qing, et al. "The 2009 pandemic H1N1 neuraminidase N1 lacks the 150-cavity in its active site." *Nature structural & molecular biology* 17.10 (2010): 1266-1268.
[13] Vavricka, Christopher John, et al. "Special features of the 2009 pandemic swine-origin influenza A H1N1 hemagglutinin and neuraminidase." *Chinese Science Bulletin* 56.17 (2011): 1747-1752.
[14] Han, Nanyu, and Yuguang Mu. "Plasticity of 150-loop in influenza neuraminidase explored by hamiltonian replica exchange molecular dynamics simulations." *PloS one* 8.4 (2013): e60995.
[15] Berman, Helen M., et al. "The protein data bank." *Nucleic acids research* 28.1 (2000): 235-242.
[16] Berendsen, Herman JC, David van der Spoel, and Rudi van Drunen. "GROMACS: a message-passing parallel molecular dynamics implementation." *Computer Physics Communications* 91.1-3 (1995): 43-56.
[17] Van Der Spoel, David, et al. "GROMACS: fast, flexible, and free." *Journal of computational chemistry* 26.16 (2005): 1701-1718.
[18] Miyamoto, Shuichi, and Peter A. Kollman. "SETTLE: an analytical version of the SHAKE and RATTLE algorithm for rigid water models." *Journal of computational chemistry* 13.8 (1992): 952-962.
[19] Essmann, Ulrich, et al. "A smooth particle mesh Ewald method." *The Journal of chemical physics* 103.19 (1995): 8577-8593.
[20] Schrodinger, L. L. C. "The PyMOL molecular graphics system. 2010." *Version* 1: r1.
[21] Pettersen, Eric F., et al. "UCSF Chimera—A visualization system for exploratory research and analysis." *Journal of computational chemistry* 25.13 (2004): 1605-1612.
[22] Dundas, Joe, et al. "CASTp: computed atlas of surface topography of proteins with structural and topographical mapping of functionally annotated residues." *Nucleic acids research* 34.suppl 2 (2006): W116-W118.
[23] Gu, Yina, Da-Wei Li, and Rafael Brüschweiler. "Decoding the mobility and time scales of protein loops." *Journal of Chemical Theory and Computation* 11.3 (2015): 1308-1314.